Stray Light Correction

Introduction

Scattering by the grating is the dominant source of stray light in grating spectrometers like the Brewer MKIV. However, holographic gratings have lower stay light for higher line density. Therefore gratings of the following three Brewer models have stray light in the following descending order: MKIV, MKII, MKIII. Other sources of stray light include: (2) scattering by mirror surfaces, (3) scattering by surfaces of lenses and filters, (4) scattering by striae and inclusions in optical materials of lenses and filters, (5) multiple reflections between surfaces of lenses and filters that create weak out of focus secondary images, (6) Rayleigh and Mie scattering by air and dust particles in the air within the spectrometer, (7) scattering by housing surfaces, (8) Rayleigh scattering by the volume of glass and fused silica, (9) distortions due to thermal gradients in the air within the spectrometer, and (10) diffraction on the apertures. There are also ghosts caused by grating defects. Both the grating ghosts and specular reflections (glints) from aperture edges and optical element mounts are strongly wavelength dependent.

Due to instrument contamination with dust the stray light is expected to increase after field deployment. This may have a larger relative effect with the MKIII (in the second spectrometer of the double) with a grating that scatters less than in the MKIV with a lower groove density grating that scatters more.

The stray light results in a finite out-of-band rejection (OBR), meaning that light of other more distant wavelengths than those specified by slit function's fwhm also contributes to the signal. The finite OBR causes significant error or spectrum distortions in regions where strong absorption or emission bands occur. In UV solar spectrometry the Hartley-Huggins ozone band precipice (280nm-310nm) is particularly affected by the spectroradiometer's OBR.

If stray light is not corrected in UV scans, the calculated UV index is too large. Also, in direct sun observations (DS routine) stray light results in underestimated ozone column for larger air masses. In this document we concentrate on stray light correction in UV scans that we employed in generating 201 and higher UV scan data levels. This method may lead to a similar stray light correction of DS data. However, it was not tested prior to preparation of this document.

We show results both from simulations and statistical summary from stray light corrections of actual data from eight network Brewers.

Spectrometer integral equation

Mathematically speaking - it can be shown – that a spectrometer acts as a linear integral operator

Prepared by: P. Kiedron, P. Disterhoft and K. Lantz

$$C(p)=\int I(\lambda)r(\lambda)S(p,\lambda)d\lambda \tag{1}$$

that maps a quasi-monochromatic (fwhm≈0) irradiance $I(\lambda)$ onto the electrical signal (or counts) $C(p)$, where: (1) p is the grating position and it is expressed in units of wavelength, (2) $r(\lambda)$ is the quasi-monochromatic responsivity, and (3) $S(p,\lambda)$ is the filter function as a function of λ and the slit scattering function as a function of p. The filter functions are normalized:

$$\int S(p,\lambda)d\lambda=1 \text{ for every } p \tag{2}$$

In detector array spectrograph based spectroradiometer a snapshot of a spectrum for all wavelengths is taken simultaneously. Then eq. (1) in principle can be solved with respect to $I(\lambda)$ or in other words, a perfect stray light correction is possible. The stray light correction via the solution of eq. (1) was described and used for detector array based spectroradiometer (RSS) in Kiedron et al. (2002). See also Seim and Prydz (1972), Brown et al. (2003) and Zong et al. (2006) for matrix based methods.

Note 1: The stray light effect is zero if $I(\lambda)r(\lambda)$=const. Consequently, by selecting a responsivity that produces smaller variance in $r(\lambda)I(\lambda)$ reduces the stray light effect. In UV-RSS the stray light is reduced by using dynamic range compressing fore-optics (Kiedron et al. 2001) and in VIS-RSS two color glass filters are used for the same purpose. (Kiedron et al. 2002). The dynamic range reduction approach is achieved at the cost of lowering the signal-to-noise ratio.

In a scanning spectroradiometer like the Brewer irradiance changes during a scan. For each grating position p the irradiance $I(\lambda)=I_p(\lambda)$ as the sky is different at different instances of p (the position p is a linear function of time). Thus, instead of one equation we must write a set of N equations:

$$C(p)=\int I_p(\lambda)r(\lambda)S(p,\lambda)d\lambda \, , \quad p=1,...,N \tag{3}$$

In the general case this set of equations cannot be solved with respect to N vectors $I_{p1}(\lambda)..., I_{pN}(\lambda)$ (each is N long) with only N measurement values $C(p_1),...,C(p_N)$. In the case of clear and stable sky $I_p(\lambda)$ vectors are not independent and they change with p in a regular way via sun zenith angle (SZA). Then an exact stray light correction is possible, however, it is achieved through a rather cumbersome process of irradiance extrapolation and synthesis.

Stray light in the UV scan is a dominant component of the signal $C(p)$ at the shortest wavelengths. Thus the level of stray light can be estimated directly in each UV scan and its value is $C(p)$ at p for which the irradiance is practically zero. Accurate characterization of an instrument, i.e. knowledge or $r(\lambda)$ and $S(p,\lambda)$ functions is then not needed. The value of the stray light can be subtracted from the signal. This amounts to a partial stray light correction. The efficacy of this approach is evaluated with simulations in the next section. We also analyze the role of stray light in ozone retrieval.

Simulations of stray light and its correction

We use eq. (1) to perform stray light simulations and estimate the quality of stray light correction. To perform simulations we must estimate the quasi-monochromatic responsivity and filter functions.

In Figure 1 filter functions *S(p,325nm)* obtained with a HeCd laser for two MKIV Brewers are depicted. The difference between BR101 and BR114 as seen in Figure 1 was confirmed with other measurements implying that a 0.5 order of magnitude difference in the slit scattering function exists between seemingly identical Brewers.

Note 2: It should be noted that the 1200 lines/mm holographic grating in the MKIV produces higher stray light than higher line density gratings of the MKII and MKIII Brewers. A ruled grating of the same line density would be expected to still have an order of magnitude larger stray light.

For simulations we use the two slit scattering functions from Figure 1. We assume that for other than 325nm wavelengths slit scattering functions have the same wings. The central part of the function however is replaced with triangular functions of fwhm that changes according to the anamorphic magnification of the Brewer spectrometer.
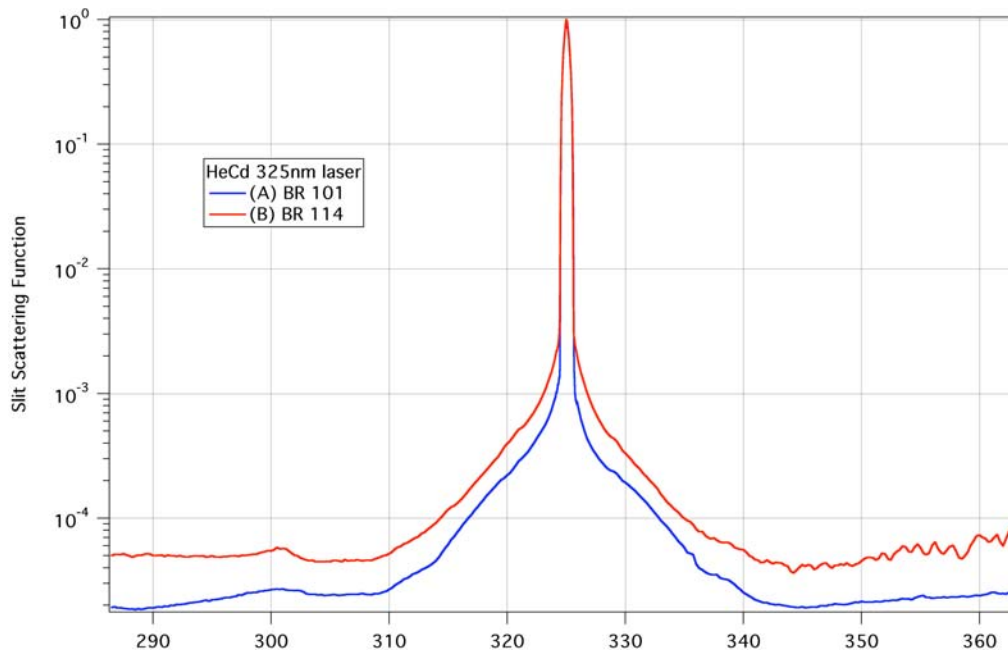

Figure 1. Slit scattering functions for two Brewers measured during 1997 Intercomparison of Ultraviolet Monitoring Spectroradiometers (Lantz et al. 2002) (data from: ftp://ftp.srrb.noaa.gov/pub/data/CUCF/).

The fwhm as a function of wavelength (green trace in Figure 2) is an approximation. In fact the fwhm most likely has a discontinuity at 325nm where the slit is changed during

the UV scan. However exact values of the fwhm have a rather negligible impact on stray light simulations.

Note 3: Many of the fwhm values for Hg, Cd and Zn spectral lines in Figure 2 are significant outliers. This is because some lines are not singlets and because of errors due to the inadequate sampling density. The data points for Figure 2 were taken from the 1997 Inte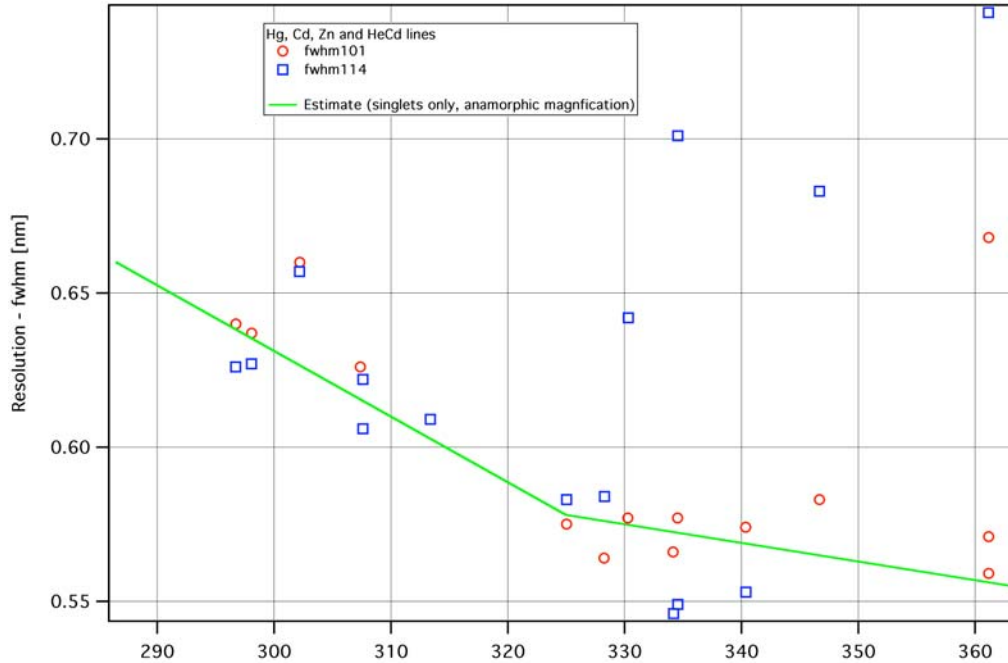rcomparison of Ultraviolet Monitoring Spectroradiometers (ftp://ftp.srrb.noaa.gov/pub/data/CUCF/) without additional screening.

Figure 2. Brewer MKIV approximate resolution (fwhm) as a function of wavelength (green trace).

To reduce the effects of stray light the Brewer MKIV employs a solar blind filter (SBF) made of nickel sulphate hexahydrate ($NiSO_4 \cdot 6H_2O$) crystal sandwiched between two UV colored glass like Schott's UG5 or UG11 (we do not know the exact glass used). The SBF blocks longer wavelengths from entering the PMT's cathode. The SBF is employed during the UV scan for $\lambda < 325nm$ and during DS measurements.

Note 4: The nickel sulphate based SBF has two leaks: 1% at 465nm and 6% at 895nm. The latter should not cause problems as the cathode of the PMT used by the Brewer seems to have zero quantum efficiency in the near IR. The 465nm leak, however may contribute to stray light during measurements. A separate test would have to be performed to verify it. In our simulations we ignore this leak by setting $r(\lambda)=0$ for $\lambda > 363nm$.

In Figure 3 responsivities for $p < 325nm$ obtained using a lamp of known irradiance $I_{lamp}(\lambda)$ are depicted. These responsivities are obtained from measured counts

$$C_{lamp}(p) = \int I_{lamp}(\lambda) r(\lambda) S(p,\lambda) d\lambda \qquad (4)$$

as follows

$$R_{lamp}(p)=C_{lamp}(p)/I_{lamp}(p) \qquad\qquad (5)$$

For simulations we estimated the responsivity beyond 325nm based on SBF's transmittance.
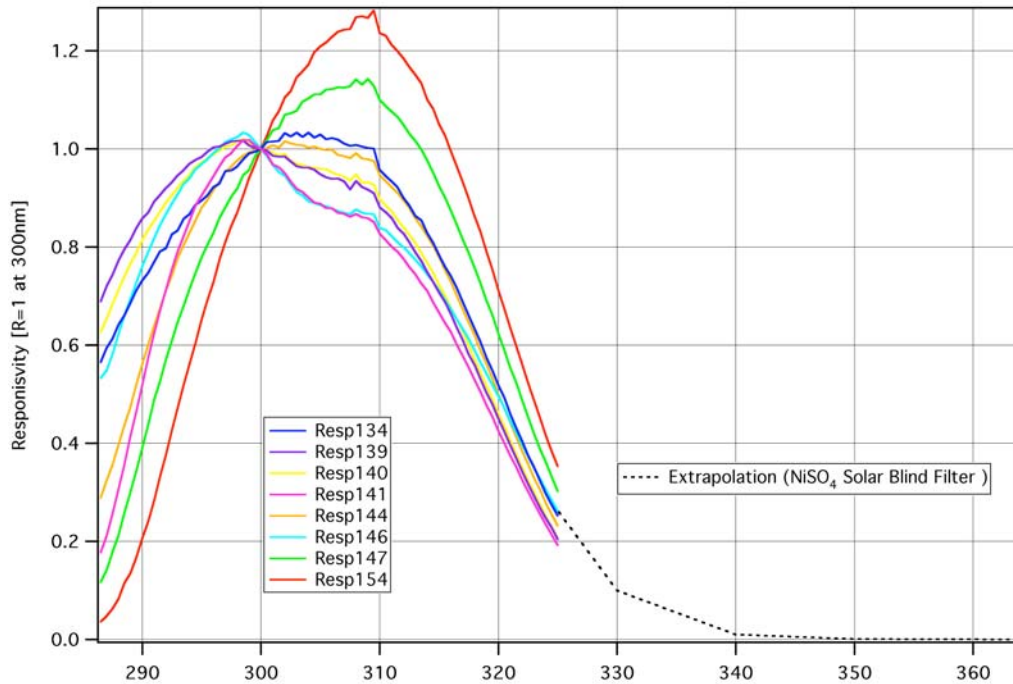

Figure 3. Normalized responsivity measured with CUCF lamps in 286.5nm-325nm range and extrapolated responsivity in 325nm-363nm range based on the transmittance of the $NiSO_4$ filter.

Note 5: The responsivity of Brewer 154 (red) is expected to lead to higher stray light effect than the responisvity of Brewer 139 (violet).

Stray light in responsivity

The lamp based responsivity eq.(5) is affected by stray light. To obtain a quasi-monochromatic responsivity $r(p)$ one would have to solve eq.(4) or in other words remove the stray light from $C_{lamp}(p)$ counts before applying eq.(5). The solution of eq.(1) for static irradiance (like lamp irradiance) was described and used for array based spectroradiometers (RSS) in Kiedron et al. (2002).

For simplicity sake of our simulations instead of inverting the integral eq.(4) we set $r(p)=R_{lamp}(p)$ (where $R_{lamp}(p)$ are from Figure 3) and then obtain the new $R_{lamp}(p)$ using eqs. (4) and (5). The lamp irradiance $I_{lamp}(\lambda)$ of a typical CUCF lamp (see Figure 4) was used in eq.(4) to obtain the new $R_{lamp}(p)$.
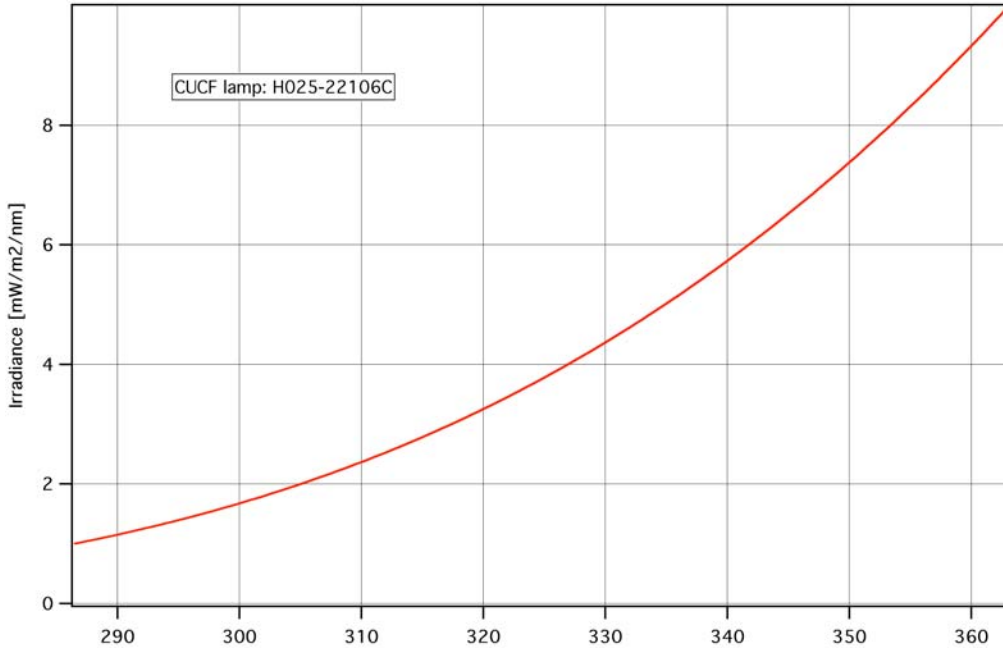

Figure 4. Typical irradiance of CUCF FEL lamp.

In Figure 5 we show the ratio of two responsivities: $R_{C+W}(p)/R_C(p)$, where $R_C(p)$ was calculated assuming filter functions that have only central (C subscript) parts non-zero as triangular functions with a fwhm according to Figure 2. And $R_{C+W}(p)$ was calculated using filter functions with the same central part C and with wings W from slit scattering functions in Figure 1 for the two cases A and B. Calculations were done for all responsivities from Figure 4 were considered as quasi-monochromatic responsivities in eq. (4). As expected (see Note 5) Brewer 154 has the largest stray light effect and Brewer 139 has one of the lowest. A less intuitive result is that a responsivity with stray light is lower than a responsivity without stray light in the region where a quasi-monochromatic responsivity is maximum. One possible explanation for this is that the filter function dissipates energy into its wings, which results in a reduced value of the signal $C(p)$ where $r(\lambda)I(\lambda)$ has its maximum ($p=\lambda$) in eq. (4).
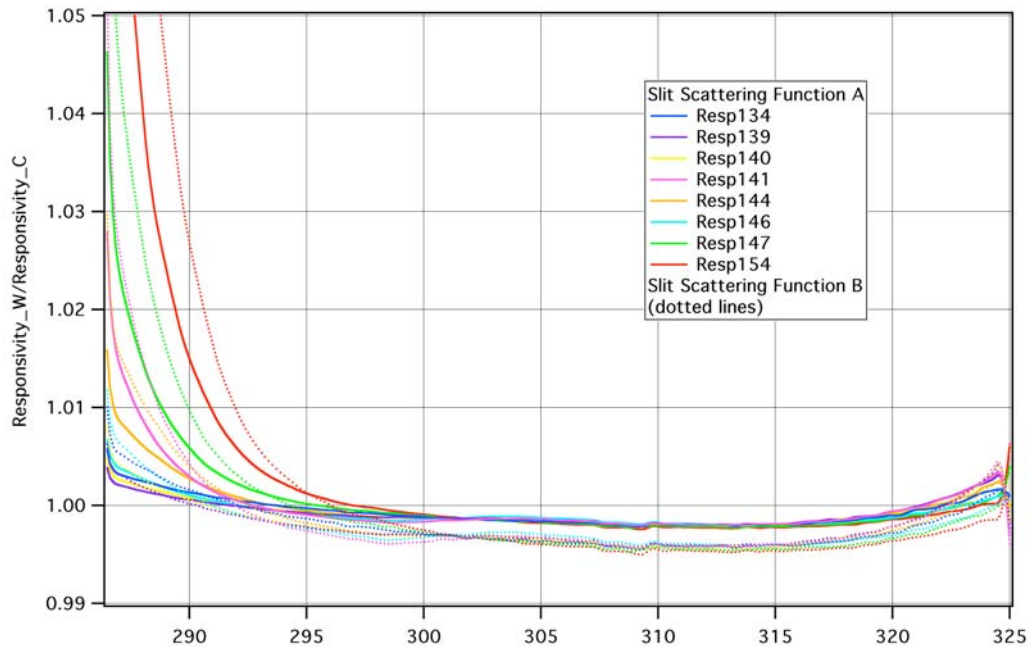
Figure 5. Ratio of the responsivity with stray light to the responsivity without stray light for eight different quasi-monochromatic responsivities and two slit scattering functions.

The results in Figure 5 indicate that without an accurate characterization of an instrument that would allow correction of stray light, stray light in the responsivity alone may cause systematic errors of ±0.3% in the 295nm-325nm region.

<u>Stray light effect in ozone retrieval</u>

During the DS measurement routine the direct sun irradiance is measured at five wavelengths via five separate slits (i=2,...,6) at one grating position:

Table 1. Brewer nominal slit values

i	0	1	2	3	4	5	6
λ_i	303.2	dark	306.3	310.1	313.5	316.8	320.1
fwhm		n/a	≈0.6	≈0.6	≈0.6	≈0.6	≈0.6

From eq.(1) we calculate irradiance signals $C(\lambda_i)$ using as input N=1000 irradiances

$$I(\lambda)=I_0(\lambda)exp[-x(\lambda)DUm_{o3} - r(\lambda)m_r - a(\lambda)m_a] \qquad (6)$$

where:

$I_0(\lambda)$ – is the extraterrestrial irradiance (Bernhard et al. 2004)
$x(\lambda)$ – is the Bass-Paur ozone cross-section at 229K
DU – ozone column: random uniform in [150DU-450DU]
$r(\lambda)$ – Rayleigh optical depth: random pressures P in [850mb-1050mb]

$$r(\lambda[\mu m]) = 0.008569\lambda^{-4}(1+0.0113\lambda^{-2}+0.00013\lambda^{-4}) \cdot (P/1013) \tag{7}$$

$a(\lambda)$ – aerosol optical depth is linear with wavelength:

         $a(286.5)$ random in [0.01OD-1.01OD]

         $a(365.0) = k \cdot a(286.5)$, where is k random uniform in [0.5-1.0]

E – solar elevation angle: random uniform in [0°, 88°]

and the air masses are calculated from the following standard equations:

m_{o3} – ozone air mass for $h=22km$, $R=6370km$

$$m_{o3} = (1+h/R)/(sin^2(E) + 2h/R)^{0.5} \tag{8a}$$

m_r – Rayleigh air mass

$$m_r = (sin(E)+0.50572(6.07995+E°)^{-1.6364})^{-1} \tag{8b}$$

m_a – aerosol air mass

$$m_a = (sin(E)+0.0548(2.650+E°)^{-1.452})^{-1} \tag{8c}$$
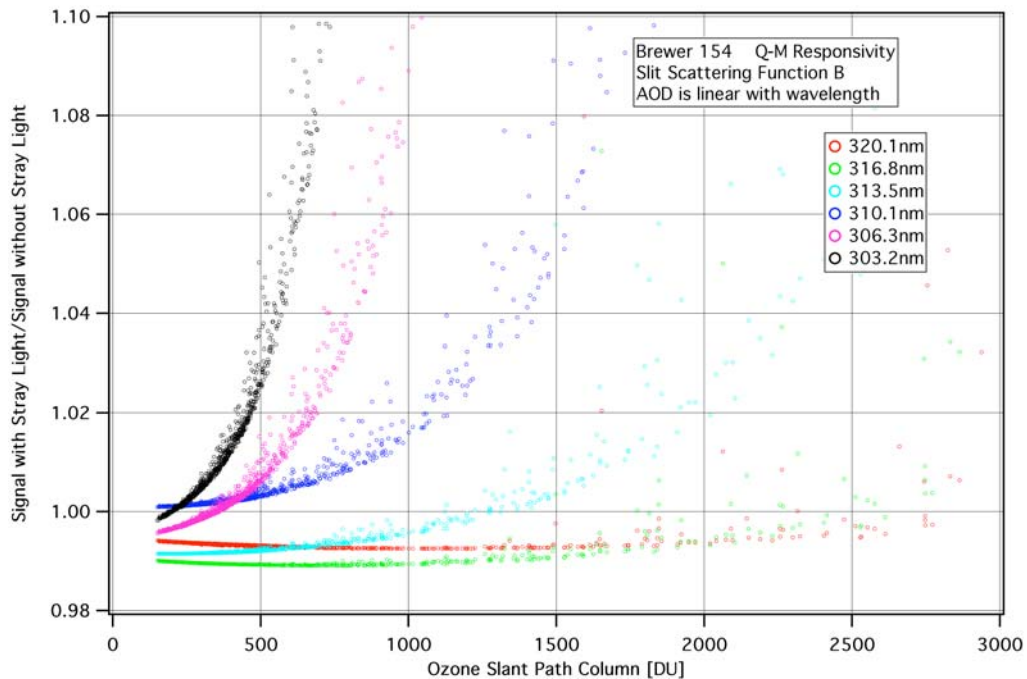
Figure 6. Ratio of the signal with stray light to the signal without stray light for BR154 at six wavelengths (slit scattering function B).

In Figure 6 the ratios $C_{C+W}(\lambda_i)/C_C(\lambda_i)$ show the magnitude of stray light for six wavelengths from Table 1.

Ozone absorption is a chief cause of stray light effect. The smallest air masses lay along the lower envelopes of the scattered points in Figure 6. The points that lay about these curves are for cases of lower ozone values but large air masses. For large air masses Rayleigh extinction becomes a significant contributor to the stray light effect.

The four longest wavelengths are used to retrieve ozone. According to the Brewer algorithm irradiance signals $C(\lambda_i)$ for i=3,…,6 are used. The following quantities are calculated for the four wavelengths:

$$F_i = log_{10}C(\lambda_i) + r(\lambda_i)m_r \qquad (9)$$

To replicate pressure uncertainty, as the Brewer uses only a nominal pressure for a given site, we have added a ±5mb pressure uncertainty when calculating $r(\lambda_i)$ for eq. (9).

Ozone column DU is calculated from a linear equation:

$$DUm_{o3}=XSC(X - ETC) \qquad (10)$$

where

       XSC - is the ozone cross-section constant (<u>calculated</u>)
       ETC - is the extraterrestrial constant (<u>measured</u>)
       m_{o3} - is the ozone air mass

and X is a linear combination of measured signal irradiances:

$$X=a_1 \cdot (F_5-F_3) + a_2 \cdot (F_5-F_4) + a_3 \cdot (F_6-F_5) \qquad (11)$$

where the coefficients $a_1=1$, $a_2=-0.5$ and $a_3=-1.7$ are suppose (see Brewer manual) to make the retrieval independent of extinctions that are linear with wavelength (chiefly aerosols).

> Note 6: Both coefficients *XSC* and *ETC* could be obtained using the correlation technique from another Brewer that is collocated and calibrated. This would be a transfer of calibration. In such a case the Brewer under calibration becomes a <u>secondary</u> instrument. When *XSC* is calculated from characterization data of the Brewer, and the *ETC* is obtained from Langley regressions (DU is unknown but must be constant in eq.(10) in the Langley plot), then the Brewer under calibration will measure ozone from the first principles. We think it is very important to make a distinction between <u>secondary</u> and <u>first principles</u> instruments.

XSC can be calculated explicitly using ozone x-sections and values of wavelength λ_i. *XSC* can also be obtained implicitly from simulations like we have done here (see Figure 7). In Figure 7 two simulated Langley plots are depicted. The coefficients *XSC* and *ETC* are obtained by fitting all of the points with an ozone slant path column $DU \cdot m_{o3}$ less than

1100DU. One can see that stray light affects *XSC*. *XSC* and *ETC* are different for the two cases.
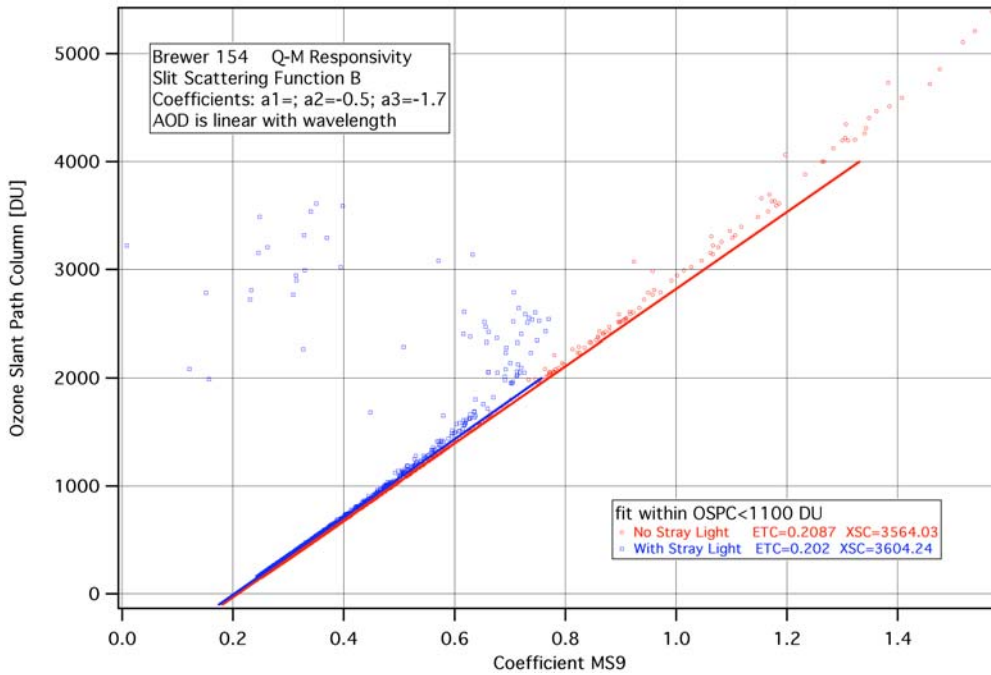

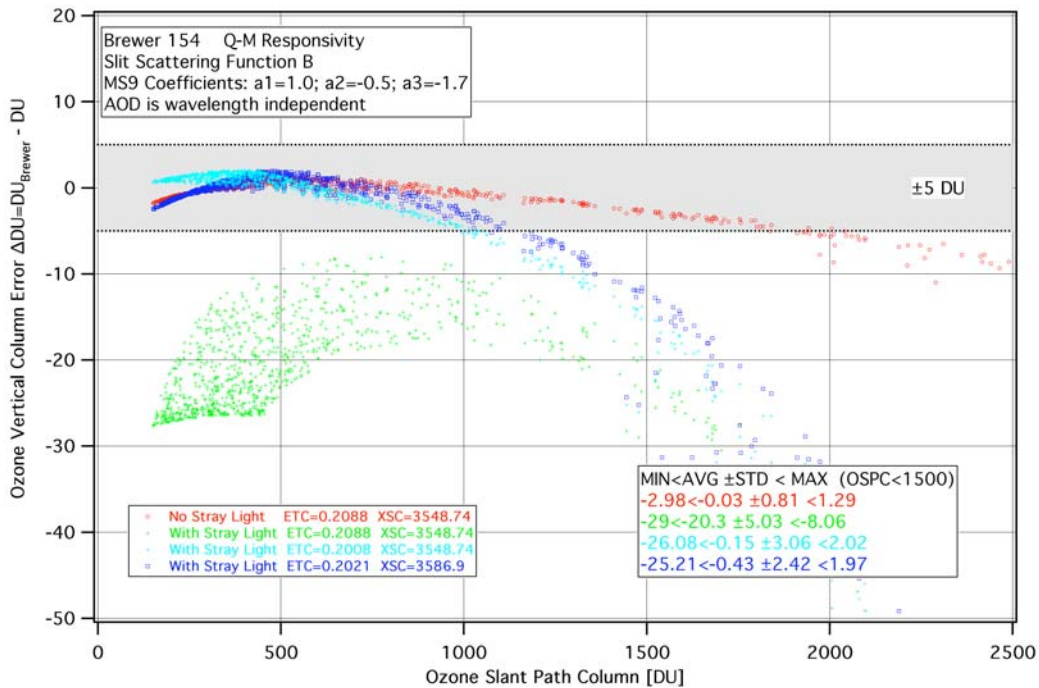Figure 7. Ozone Langley plots to determine *XSC* and *ETC* coefficients.

Figure 8. Ozone column retrieval errors in four cases. AOD is wavelength independent.

In Figures 8 we show ozone retrieval errors, i.e., difference between ozone DU_{Brewer} obtained from eq.(10) and ozone DU used in eq.(6) to calculate X with eq.(11). In this case aerosols are assumed to be wavelength independent. Four possibilities are shown: (red) retrievals when the data had no stray light; (green) *XSC* and *ETC* parameters used from red case for data with stray light; (light blue) only *XSC* from the red case was used and the *ETC* was adjusted using data with stray light; and (blue) both *XSC* and *ETC* were determined from data with stray light.

We can conclude that *XSC* does not need to be determined using stray light data in the calculations (light blue); however a small improvement is gained if it is (blue). The stray light significantly reduces retrieved ozone column. At 1500DU slant path ozone column a -26DU error is expected. Furthermore, we are somewhat surprised that in the no stray light case there is also a dependence on ozone slant path column (red).

In Figure 9 wavelength dependent aerosol optical depths was added in simulations.
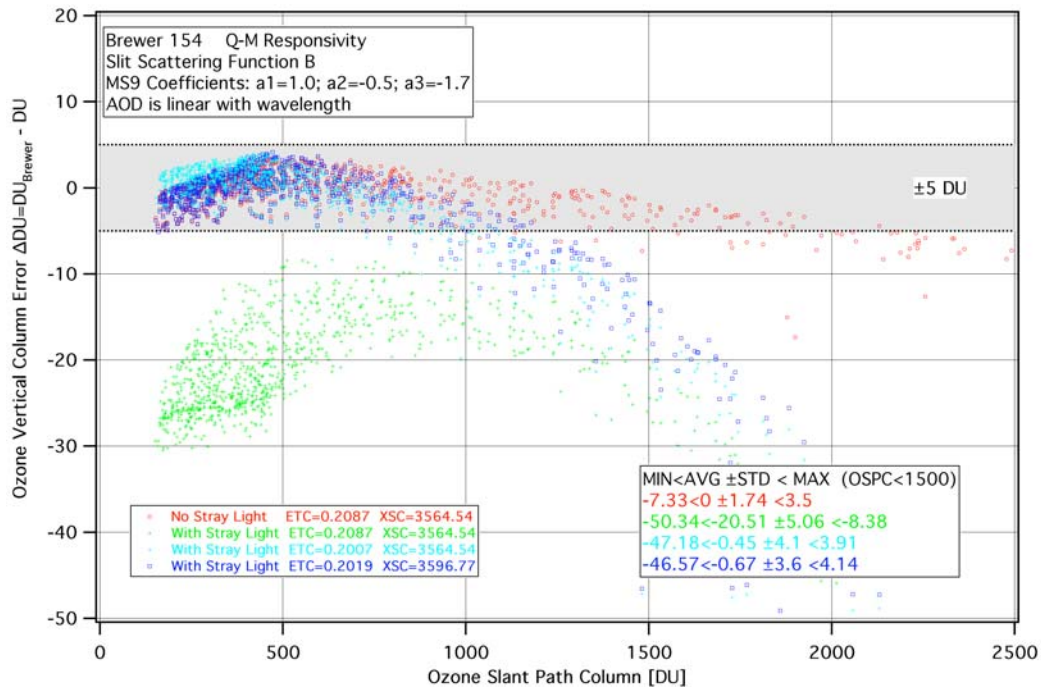
Figure 9. Ozone column retrieval errors in four cases. AOD is linear with wavelength.

On p.113 of the Brewer manual it is stated that "weightings [a_2=-0.5 and a_3=-1.7 in eq.(11)] remove the effects of absorption which are linear with wavelength". Figure 9 clearly does not concur. Perhaps because in our simulations we did not have exactly the same filter functions (λ_i and $fwhm_i$) as used by the Brewer and that we could have had an additional wavelength shift error in the Bass-Paur spectrum with respect to what the Brewer is suppose to use.
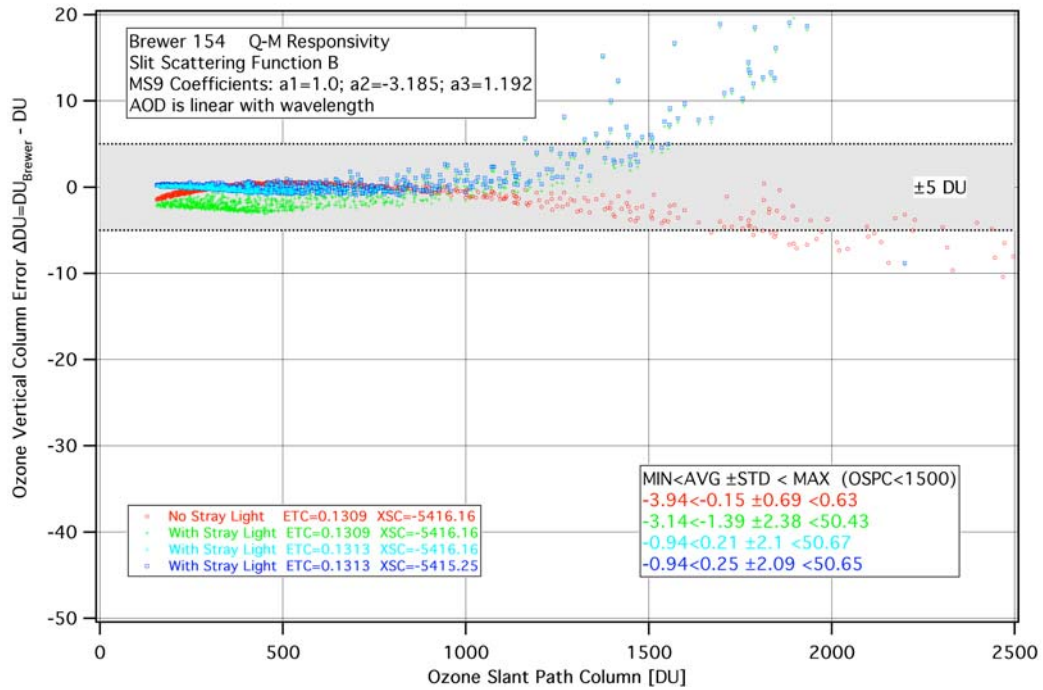
Figure 10. Ozone column retrieval errors in four cases (a_2=-3.185 and a_3=1.192).
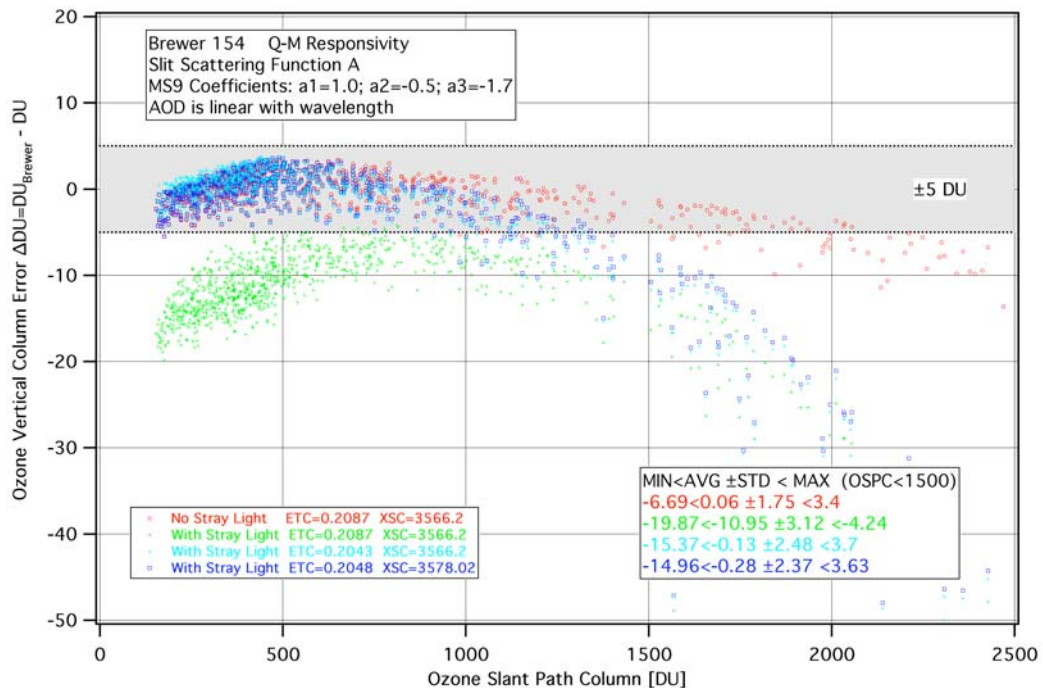

Figure 11. Ozone column retrieval errors in four cases (slit scattering function A).

In Figure 10 we demonstrate that proper selection of a_i coefficients in eq.(11) may reduce

retrieval errors. In this case Langley curves have negative slopes (*XSC* is negative). But the errors of retrievals are greatly reduced. One should not jump to a conclusion and change the weighting factors in eq. (11); however we entertain the possibility that there is room for improvement in the Brewers by better utilization of the Brewer measurement data.

As far as the stray light is concerned in ozone retrievals, our conclusion is that the slant path ozone column should not be larger than 1500DU for MKIV Brewers. Using a lower stray light level (slit scattering function A) shows only a negligible reduction of ozone retrieval errors (see Figure 11).

Stray light correction in UV scans

Lamp calibrated irradiance from level 101 $I_{101}(\lambda)$ data is used to obtain stray light corrected irradiance $I_{201}(\lambda)$ for level 201 data. Out of 67 $I_{101}(\lambda_i)$ values from $\lambda_1 = 287$nm to $\lambda_{67} = 320$nm we calculate the average of the 15 smallest values. This is the value for stray light (SL) for a given UV scan. Then the level 201 irradiance is defined as follows:

$$I_{201}(\lambda) = I_{101}(\lambda) - SL \tag{12}$$

We define the cut-on wavelength λ_c as the shortest wavelength for which all $I_{201}(\lambda) > 0$ for $\lambda > \lambda_{cuton}$. Then for all $\lambda \le \lambda_{cuton}$ we set $I_{201}(\lambda) = 0$. Also we calculate the stray light level SLL as SL divided by the average of $I_{201}(\lambda)$ in 327nm-363nm interval.

The result of the process is illustrated in Figure 12 where simulated data were used.

We note that $I_{101}(\lambda)$ has a minimum. This means that values closest to the beginning of the scan are not the smallest. This is the reason for our approach of finding the 15 smallest values in the interval instead of using the first several scan values as it is commonly done by the Brewer user community (for example see Lakkala et al. 2008 where "signal at wavelengths lower than 293nm are considered as stray light, and subtracted from longer wavelengths"). Our approach reduces overcorrection of stray light though as we show below does not eliminate it.

We have performed simulations to evaluate the efficacy of our stray light correction scheme. We used slit scattering functions A and B from Figure 1; resolution FWHM from Figure 2; quasi-monochromatic responsivities from Figure 3, stray light and stray-light-free responsivities that were used to generate Figure 5. We generated high resolution irradiance as described in previous sections. Only direct irradiance was calculated. No diffuse component was used in simulations. The sun zenith angles for each wavelength during a UV scan was obtained from sun trajectory for doy=180 at Table Mt. Colorado latitude. The summer day was selected to obtain the greatest airmass gradients within each scan. We processed morning scans and afternoon scans separately

to see the slight differences in stray light corrections when the air mass increases or decreases. A total of 5000 UV scans were simulated times two slit scattering functions, times eight responsivities and times two (AM or PM) cases. To generate one scan 154 high resolution instantaneous irradiance spectra had to be generated.
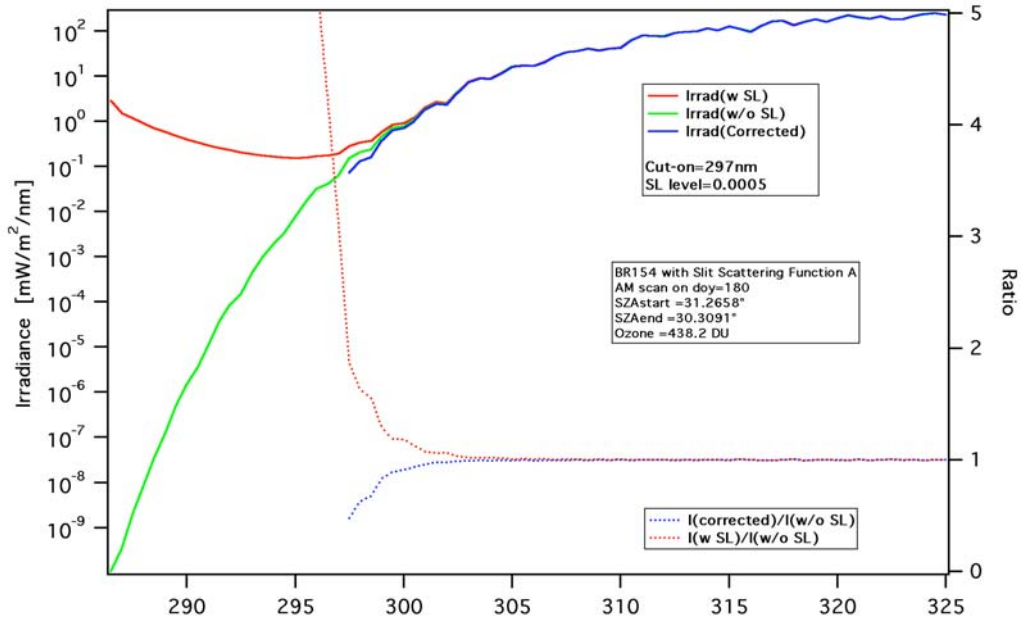

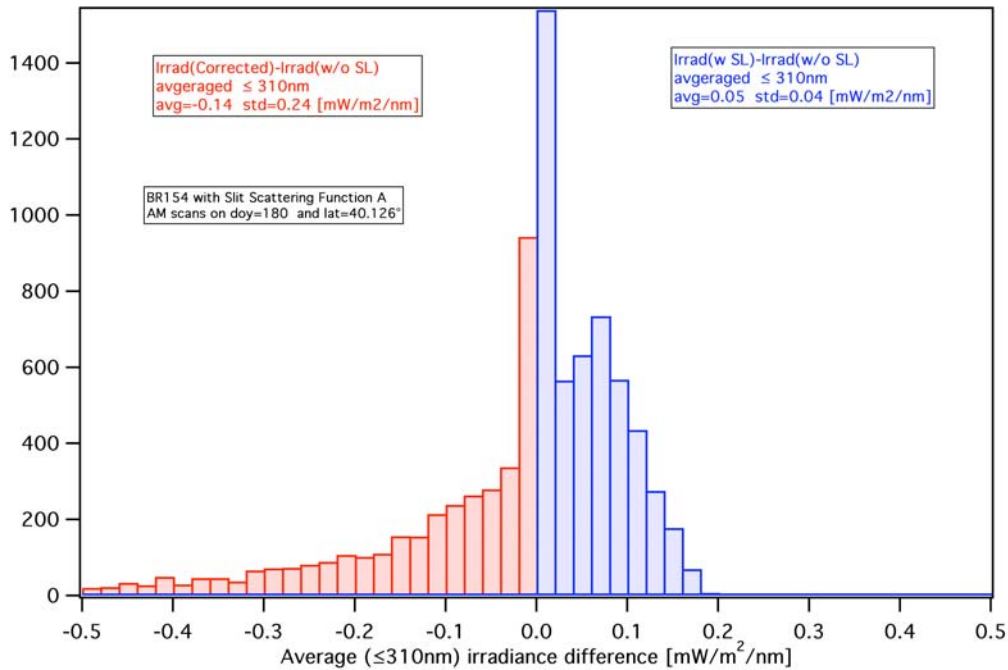Figure 12. Example of stray light correction on simulated scan.

Figure 13. Histogram of average differences between irradiances.

The correction of stray light introduces various distortions to the irradiance that are often complex and counterintuitive. To capture them for each case (1 out of 32) we calculated and plotted various measures of fidelity.

In Figure 13 we show a histogram of average irradiance differences for wavelengths between λ_c and 310nm. The result shows that corrected spectra, on average, underestimate stray-light-free spectra. The mean and standard deviations are small: -0.14 and 0.24 mW/m^2/nm, respectively.

In Figure 14 we show the mean and the standard deviations of differences for each wavelength (red curve) and show the average improvement between corrected and uncorrected spectra (blue trace). It is interesting to observe that below 295nm, on average, the irradiance with stray light overestimates stray-light-free spectrum by more than the corrected signal underestimates it. Above 295nm correction offers significant improvement. However Figure 13 and the red trace in Figure 14 show that differences in absolute irradiance are really small.
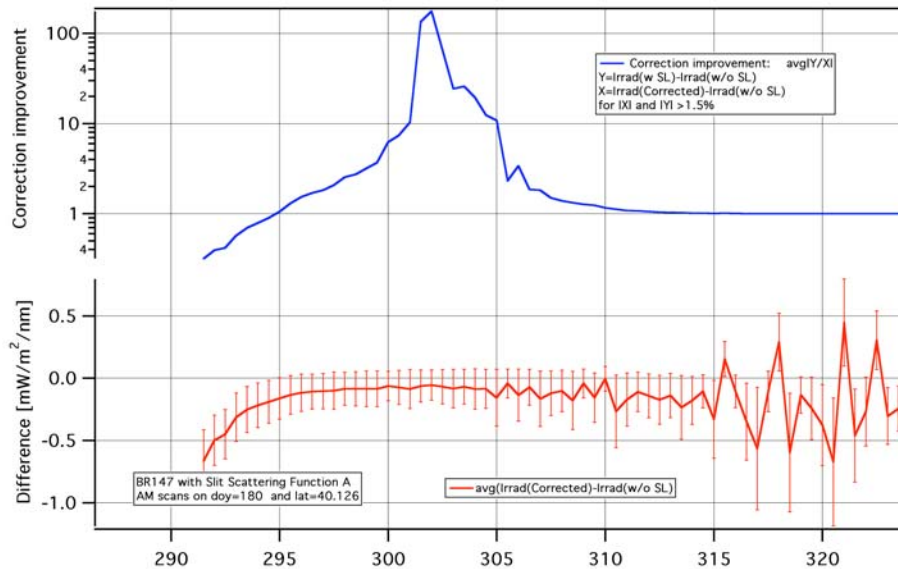
Figure 14. Average absolute differences and correction improvement.

In Figure 15 we show all 5000 differences between corrected and stray-light-free irradiances at eight wavelengths as a function of slant path ozone column. The differences are small, at most -2.5mW/m^2/nm. Also we see that at 310nm the correction was too low for many cases.
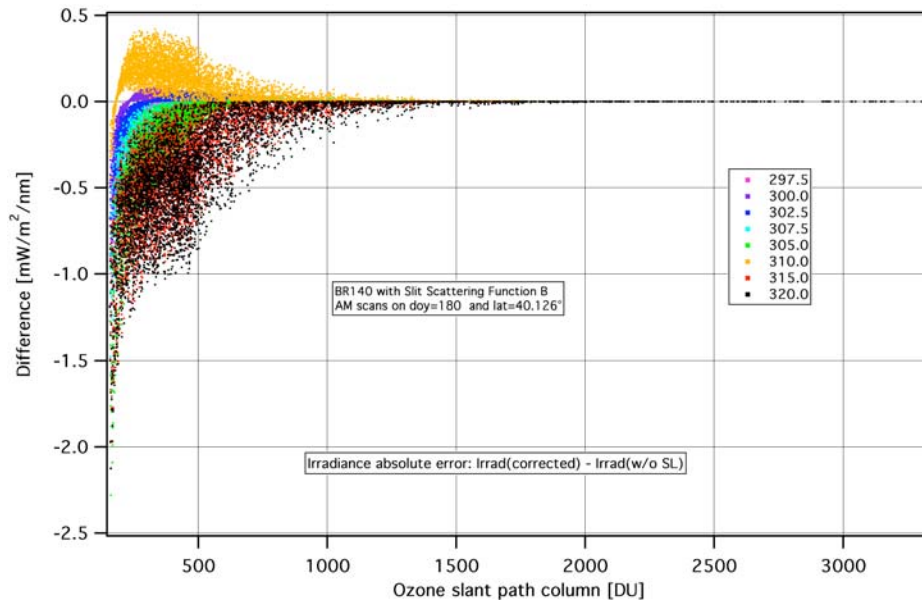
Figure 15. Absolute differences at eight wavelengths as a function of slant path ozone column (N=5000 cases).

For the same eight wavelengths we show ratios as a function of ozone slant path column in Figure 16.   We see that for large ozone slant path column and longer wavelength, overcorrection occurs and they might be as large as 50-100%. However the irradiance is then small, so there is no incongruence between Figure 15 and Figure 16. We also see that for short wavelength the traces do not extend to large slant path ozone column. This is because the cut-on wavelength gets longer as the ozone column increases.
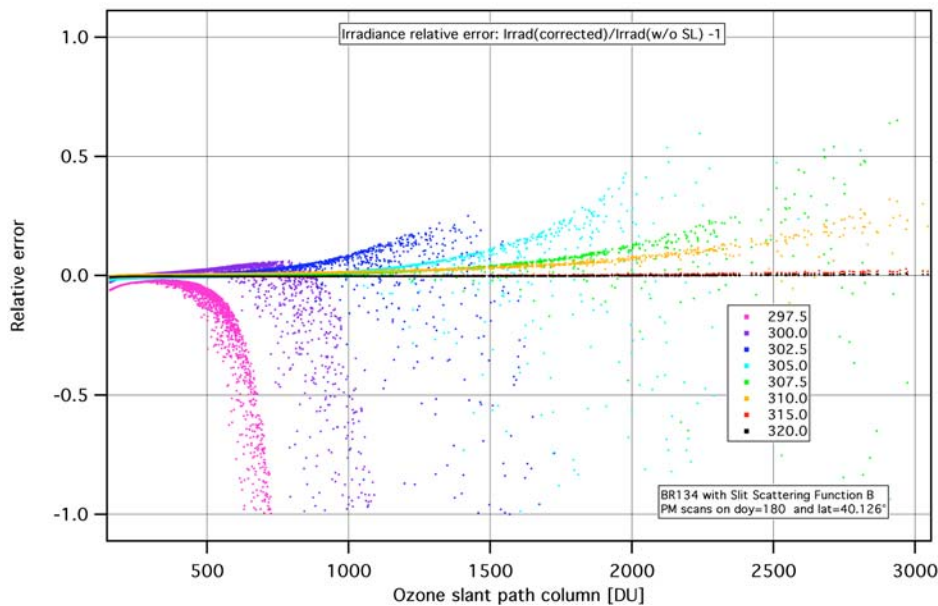
Figure 16. Relative differences at eight wavelengths as a function of slant path ozone column (N=5000 cases).
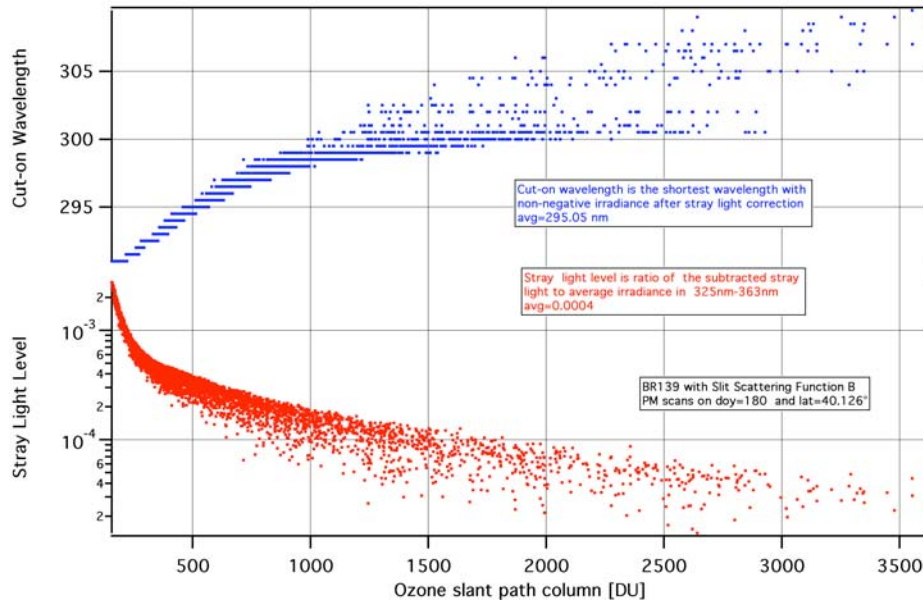
Figure 17. Stray light level and cut-on wavelength as a function of slant path ozone
column (N=5000 cases).

Figure 17 shows how stray light level and cut-on wavelength change with slant path
ozone column. It is obvious that the cut-on wavelength increases with slant path column,
but it is less obvious why the stray light level decreases.

For each case out of 32 we have generated data and Figures 13 through 17. They are not
identical but they tell the same story. We summarize the results with Figure 18 that
shows the average cut-on wavelength and stray light level (SLL) for 32 cases.

As expected the stray light level is slightly larger for PM scans than for AM scans and the
cut-on wavelengths are longer for PM scans. This summarizes the differences between
AM and PM scans and the fact that the stray light correction cannot be perfect in a
scanning instrument.

In Figure 18 we also plotted the results from Table 2 that contains the results of stray
light correction statistics run on real field data. The data, obtained from each instrument
was from 7000 to 15000 scans each. The stray light levels are within the range of
simulation results and they even correlate with simulation results. The cut-on wavelength
correlates very well.   The real responsivities from the Brewers that were used in the
simulations are responsible for the correlation. We haven't used slit scattering functions
from the fielded Brewer as they have not been measured, yet. Functions A and B in Fig.
1 are from two other Brewers.

Additional graphical results from field data stray light corrections for eight instruments
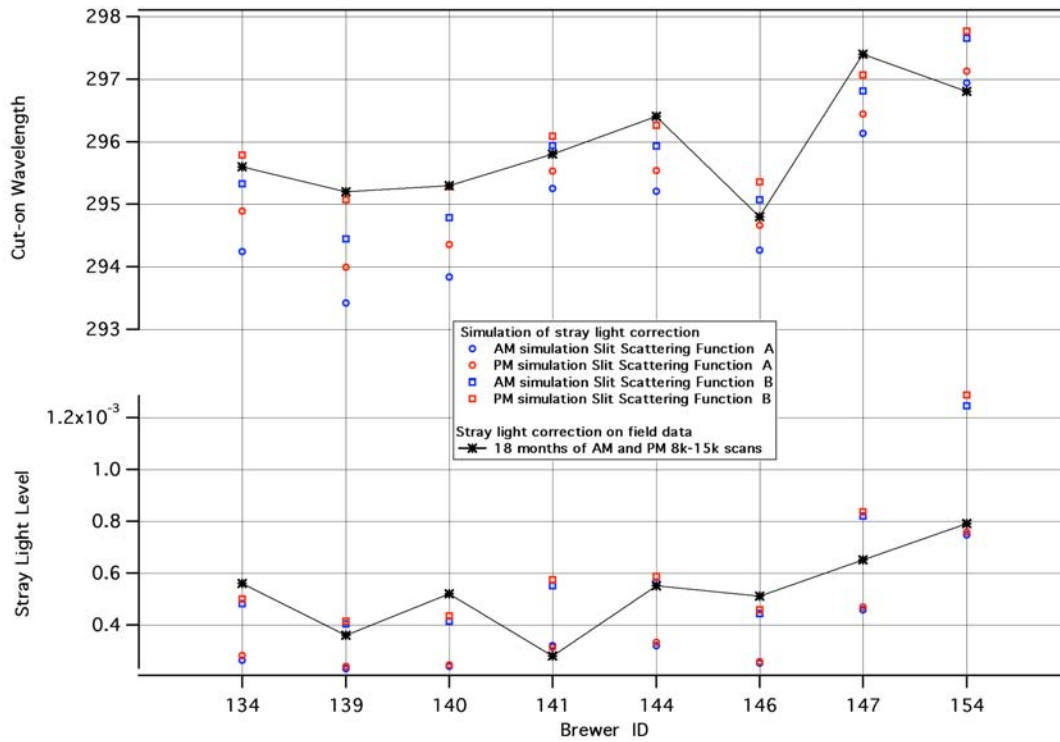are presented in the Appendix.

Figure 18. Average stray light level and average cut-on wavelength for eight Brewers, two slit scatterings, and AM and PM runs.

Table 2. Results for eight MKIV Brewers

Brewer ID	Number of UV Scans	Stray Light Fraction Average	Cut-on Wavelength λ_c Average	Noise-to-Signal at $\lambda_c +0.5$ Average
BR 134	14599	$5.6*10^{-4}$	295.6	0.967
BR 139	7417	$3.6*10^{-4}$	295.2	0.959
BR 140	15238	$5.2*10^{-4}$	295.3	0.953
BR 141	13234	$2.8*10^{-4}$	295.8	0.798
BR 144	11519	$5.5*10^{-4}$	296.4	0.849
BR 146	13465	$5.1*10^{-4}$	294.8	0.895
BR 147	12907	$6.5*10^{-4}$	297.4	0.809
BR 154	15118	$7.9*10^{-4}$	296.8	0.690

References

Bernhard, G., C.R. Booth, and J.C. Ehramjian, "Supplement to Version 2 data of the National Science Foundation`s Ultraviolet Radiation Monitoring Network: South Pole," *J. Geophys. Res.* **109**, D21207, doi:10.1029/2004JD004937, 2004

Brown, S.W., B.C. Johnson, M.E. Feinholz, M.A. Yarbrough, S. J. Flora, K. R. Lykke and D. K. Clark," Stray-light correction algorithm for spectrographs," *Metrologia* **40**, pp. S81–S84, 2003.

Kiedron, P.W, L.H. Harrison, J.L. Berndt, J.J. Michalsky, A.F. Beaubien, "Specifications and performance of UV rotating shadowband spectroradiometer (UV-RSS)," Ultraviolet Ground- and Space-based Measurements, Models, and Effects, James R. Slusser; Jay R. Herman; Wei Gao, Editors, *Proceedings SPIE* **4482** , 2002

Kiedron, P.W.; L. Harrison; J.J. Michalsky, Jr.; J.A. Schlemmer; J.L. Berndt, "Data and signal processing of rotating shadowband spectroradiometer (RSS) data," Atmospheric Radiation Measurements and Applications in Climate, Joseph A. Shaw, Editors, *Proceedings SPIE* **4815**, pp. 58-72, 2002.

Lakkala, K, A. Arola, A. Heikkil, J. Kaurola, T. Koskela, E. Kyrol, A. Lindfors, O. Meinander, A. Tanskanen, J. Grobner, and G. Hulsen, "Quality assurance of the Brewer UV measurements in Finland," *Atmos. Chem. Phys. Discuss.*, **8**, 1415–1455, 2008.

Lantz, K. , P. Disterhoft, E. Early, A. Thompson, J. DeLuisi, P. Kiedron, L. Harrison, J. Berndt, W. Mou, T. J. Erhamjian, L. Cabausua, J. Robertson, D. Hayes, J. Slusser, D. Bigelow, G. Janson, A. Beaubian, M. Beaubian, "The 1997 North American Interagency Intercomparison of Ultraviolet Monitoring Spectroradiometers," *J. Res. Natl. Inst. Stand. Technol.* **107**, 19-62, 2002.

Seim. T. and S. Prydz, "Automated spectroradiometer applying computer analysis of spectral data," *Appl. Opt.* **11**, 5, 1169-1177, 1972.

Zong, Y., S.W. Brown., B.C. Johnson, K.R. Lykke, and Y. Ohno," Simple spectral stray light correction method for array spectroradiometers," *Appl. Opt.* **45**, 6, pp. 1111-1119, 2006.

Appendix: Results for individual instruments

Graph 1 (1st from the top) shows values of stray light level for each processed scan as a function of airmass.
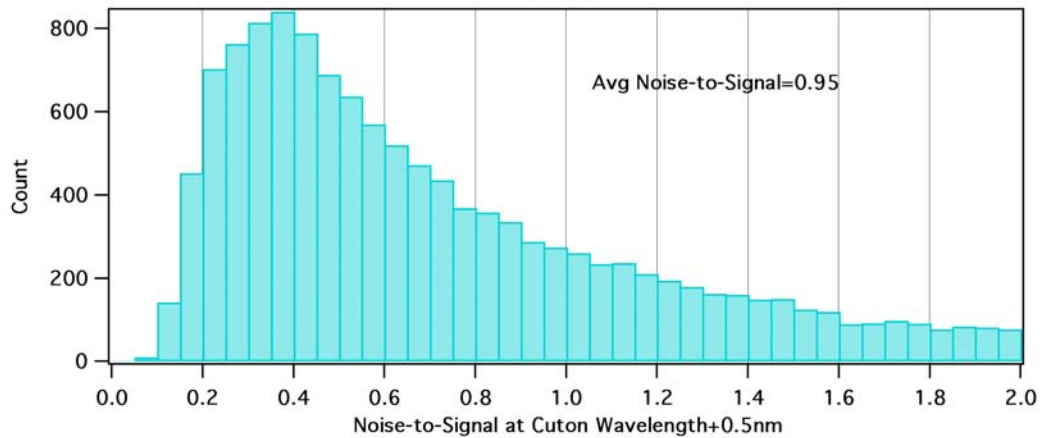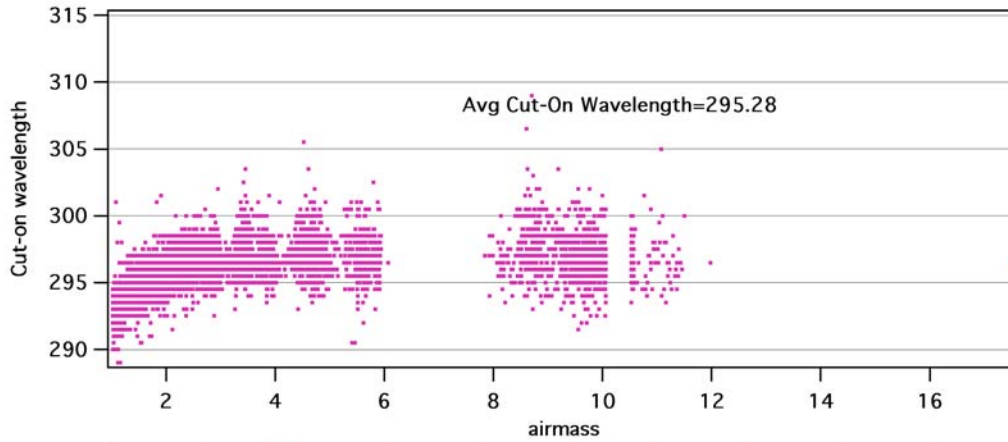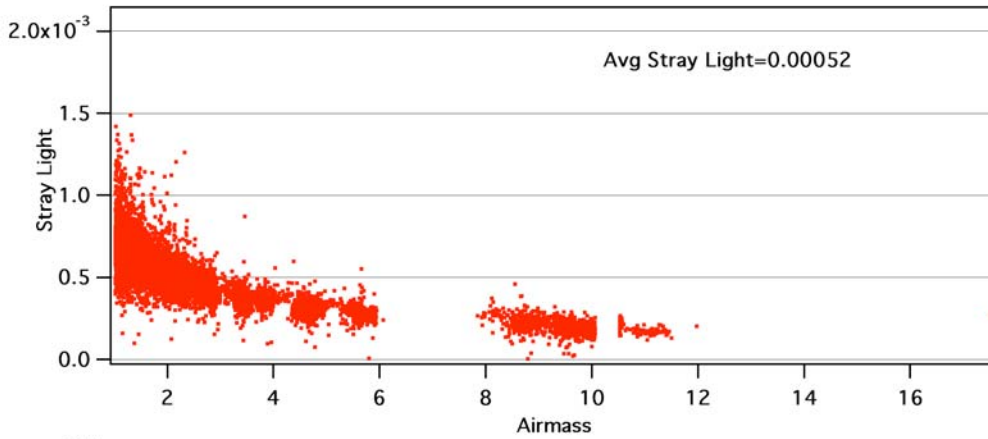
Graph 2 (2nd from the top) shows the cut-on wavelength for each processed scan as a function of airmass.

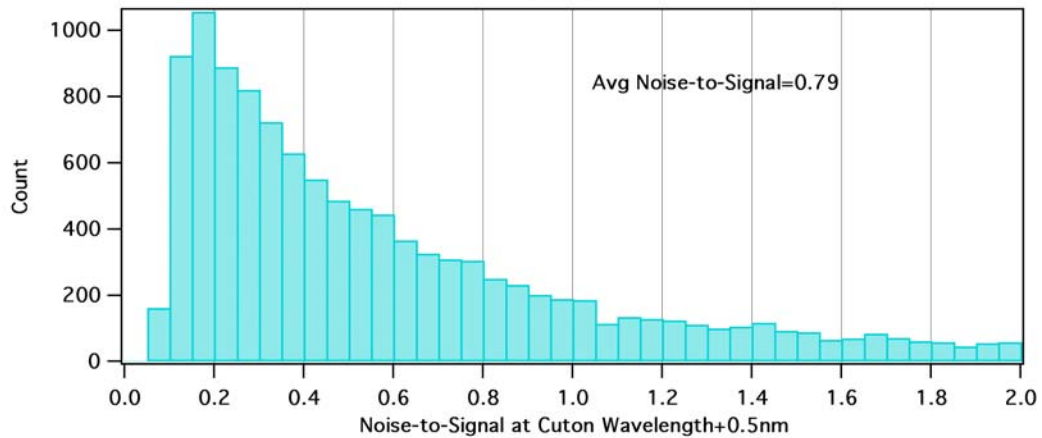Graph 3 (3rd from the top) shows a histogram of noise-to-signal for the cut-one wavelength plus 0.5nm.
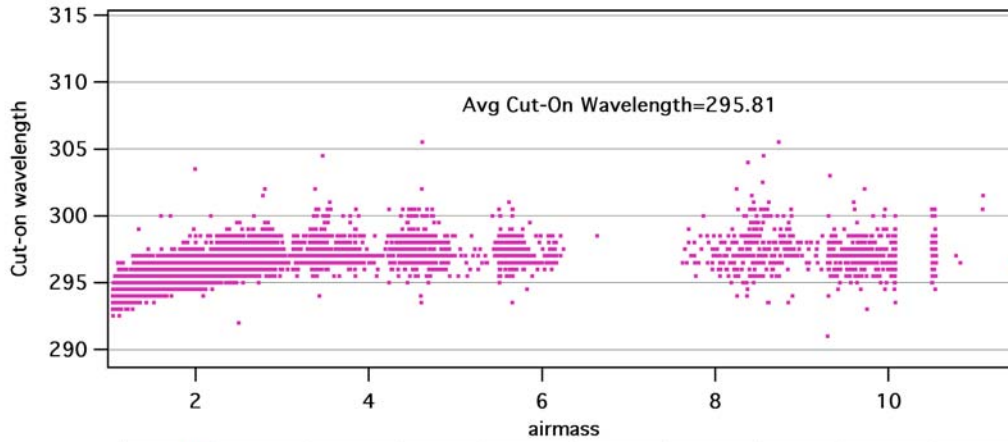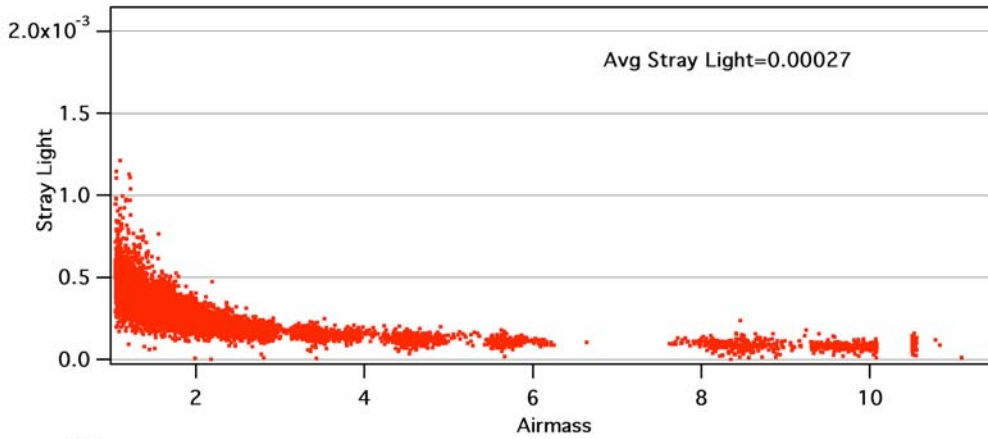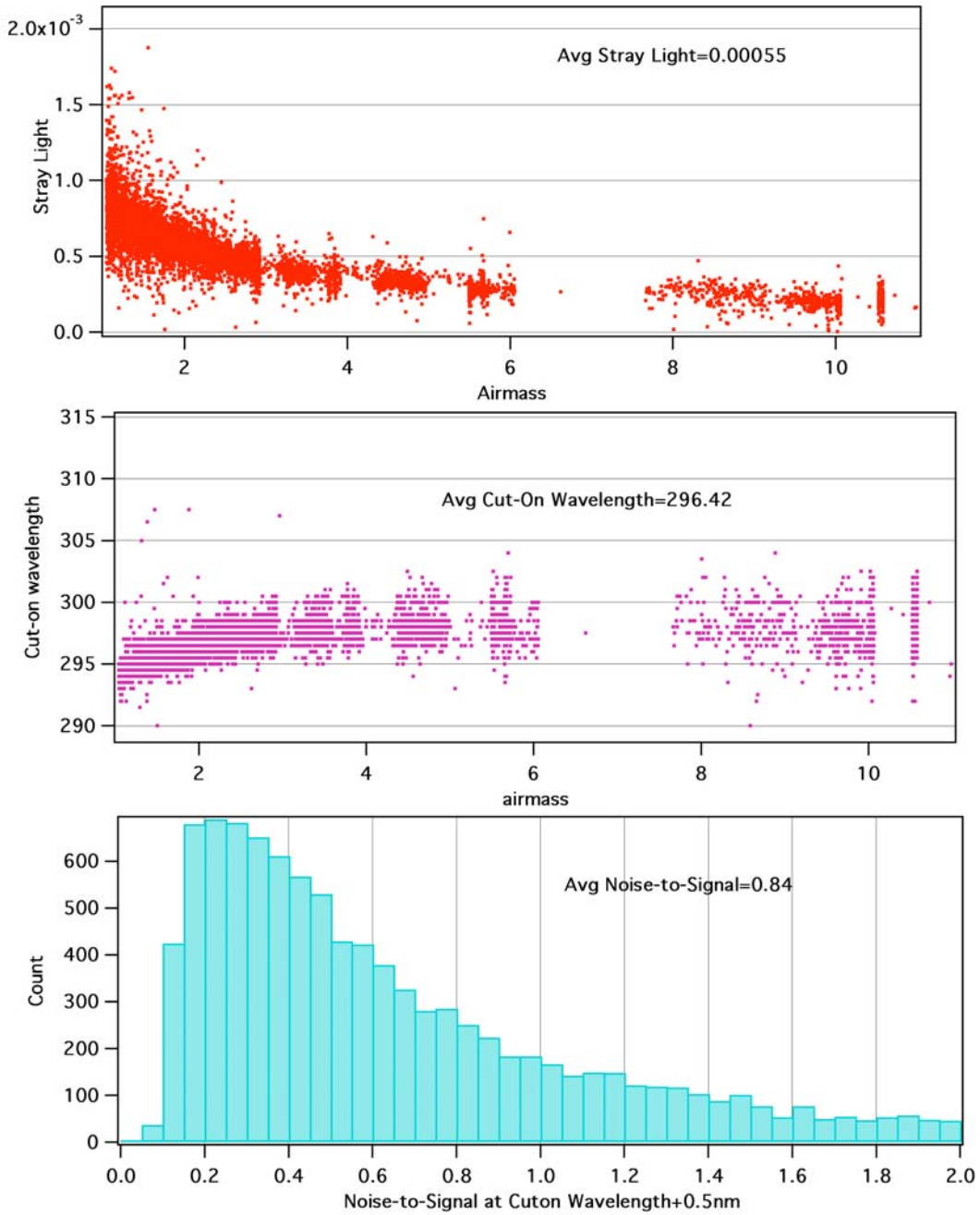
STRAY LIGHT STATISTICS 1: BR#=139
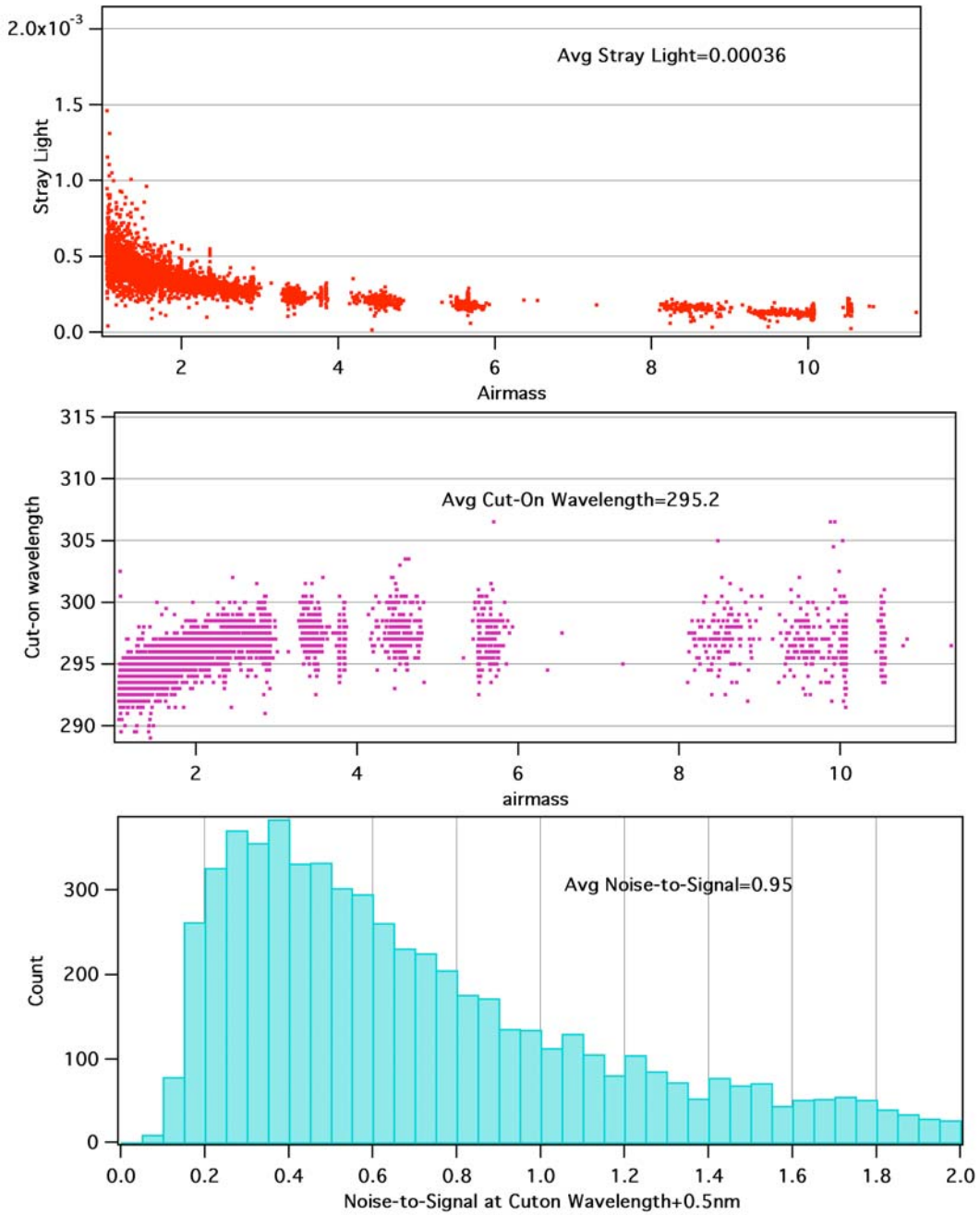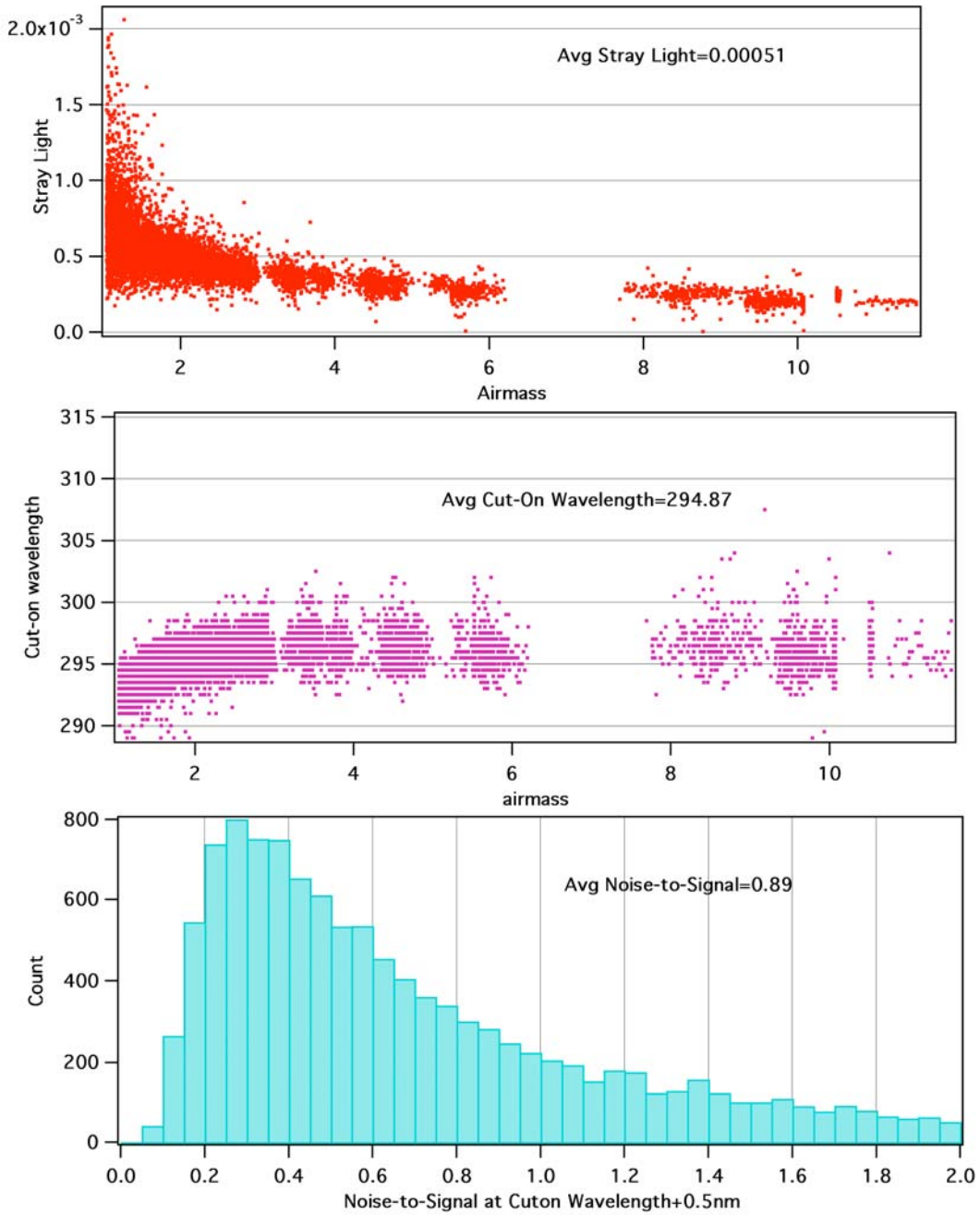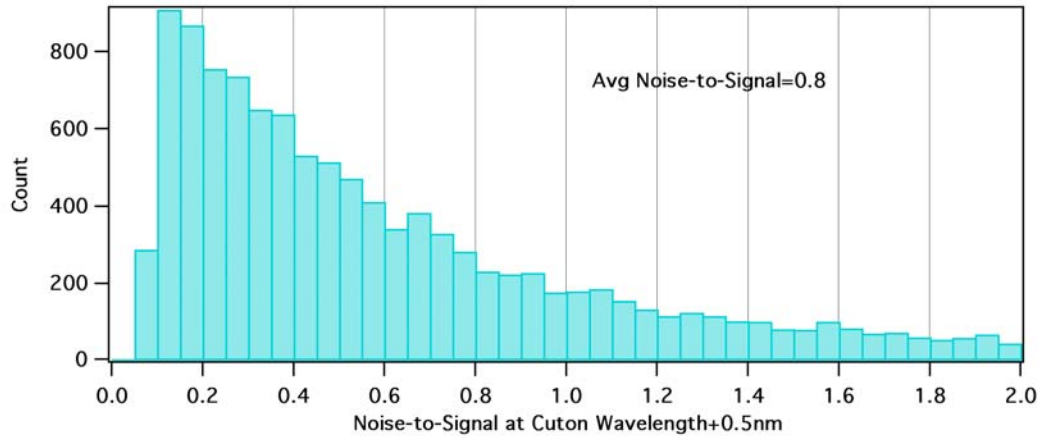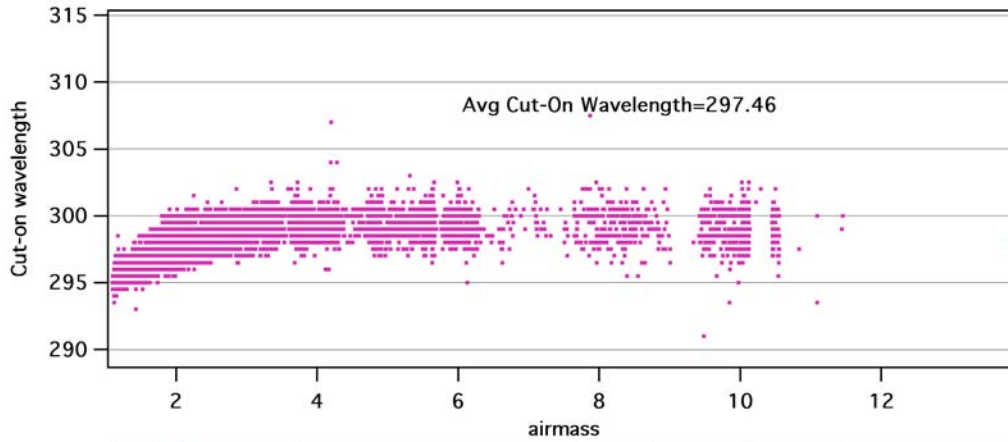
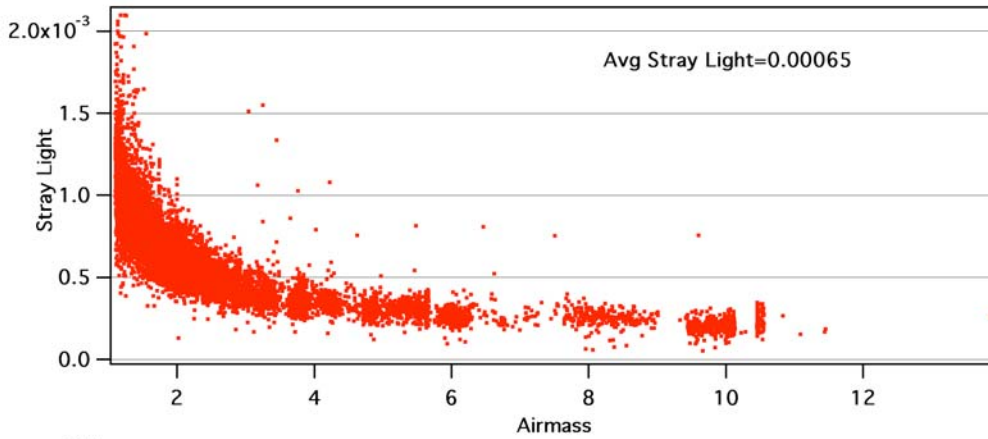STRAY LIGHT STATISTICS 1: BR#=140

STRAY LIGHT STATISTICS 1: BR#=141

STRAY LIGHT STATISTICS 1: BR#=144

Avg Stray Light=0.00055

Avg Cut-On Wavelength=296.42

Avg Noise-to-Signal=0.84

STRAY LIGHT STATISTICS 1: BR#=147

STRAY LIGHT STATISTICS 1: BR#=154

Avg Stray Light=0.00079

Avg Cut-On Wavelength=296.8

Avg Noise-to-Signal=0.69